Characterization of Interactions between a Two-Component Response Regulator, Spo0F, and Its Phosphatase, RapB†

Yih-Ling Tzeng,‡ Victoria A. Feher,§ John Cavanagh,§ Marta Perego,‡ and James A. Hoch*,‡

Division of Cellular Biology, Department of Molecular and Experimental Medicine, NX1, The Scripps Research Institute, 10550 North Torrey Pines Road, La Jolla, California 92037, and NMR Structural Biology Facility, Wadsworth Center, New York State Department of Health, Albany, New York 12201

Received June 8, 1998; Revised Manuscript Received September 8, 1998

ABSTRACT: The phosphorelay signal transduction pathway controls sporulation initiation in *Bacillus subtilis*. Transfer of a phosphoryl group from multiple kinases (KinA and KinB) through a single domain response regulator homologue (Spo0F), a phosphotransferase (Spo0B), and ultimately to a transcriptional regulator, (Spo0A) activates sporulation. Counteracting this response are phosphatases (RapA and RapB), which can short-circuit this phosphorelay via dephosphorylation of Spo0F. In vitro assays of RapB activity on phosphorylated Spo0F alanine-scanning mutants have been used to identify Spo0F residues critical for interactions between these proteins. The Spo0F surface comprised of the β1-α1 loop and N-terminal half of helix α1 has the largest number of residues in which an alanine substitution leads to resistance or decreased sensitivity to RapB phosphatase activity. Other mutations desensitizing Spo0F to RapB are also located near the site of phosphorylation on the β3-α3 and β4-α4 loops. This surface is similar to but not the same as the surface identified for KinA and Spo0B interactions with Spo0F. Divalent metal ions were shown to be required for RapB activity, and this activity was insensitive to vanadate, suggesting that Rap phosphatases catalyze acyl phosphate hydrolysis by inducing conformational changes in phosphorylated Spo0F, which results in increased autodephosphorylation. Arginine 16 of Spo0F is proposed to play a role in catalysis, and similarities between the mechanisms for RapB catalyzed Spo0F∼P hydrolysis and GAP (GTPase activating protein)-assisted GTP hydrolysis of Ras are discussed.

The initiation of sporulation in bacteria is characterized by complex interactions between signal transduction proteins that regulate the initial transcription events. A novel signal transduction system termed the phosphorelay is responsible for sporulation-related information processing (*1*). The phosphorelay is based on the two-component signal transduction systems found to be nearly universal in prokaryotes (*2*). In two component systems, a signal-activated kinase employs ATP to autophosphorylate on a histidine residue, and this phosphoryl group is subsequently transferred to an aspartate residue of a response regulator, thereby initiating a genetic or cellular response. The phosphorelay is an extended and more complex version of such a system, involving multiple activation signals processed by at least two histidine kinases, KinA and KinB (*3*). The initial target of phosphorylation is a single domain response regulator, Spo0F (*3*). Phosphorylated Spo0F (Spo0F∼P) delivers the message (phosphoryl group) to the ultimate response regulator, Spo0A, through an intermediate phosphotransferase, Spo0B, which is phosphorylated on a histidine residue during the reaction. Phosphorylated Spo0A (Spo0A∼P) is an active transcription factor controlling many genes for sporulation (*4*). Phosphorelays transfer the phosphoryl group in the order His-Asp-His-Asp and these signal transduction systems are now being found in a variety of bacteria and lower eukaryotes (*5*−*7*).

It was originally theorized that the increased complexity of the phosphorelay allowed more points of interaction for competing regulatory signals to influence the ultimate outcome of signal transduction (*1*). This is especially apparent in sporulation where a variety of environmental and cellular signals, both positive and negative, must be recognized and accommodated if the cell is to coordinate this morphological process. It is now clear that the phosphorelay forms the core of a signal integration circuit where activating signals are recognized by kinases KinA and KinB leading to phosphoryl group input and where suppressing signals regulate the Spo0E phosphatase for Spo0A∼P (*8*) and the Rap phosphatases for Spo0F∼P (*9*). In addition, an anti-kinase activity for KinA has been found (*10*). The competition between separately activated kinases and phosphatases determines the Spo0A∼P level and, therefore, whether sporulation is triggered (*11*).

Spo0F has emerged as a pivotal component in the phosphorelay as it integrates a wide variety of inputs through its interactions with three kinds of proteins: KinA and KinB kinases, the Spo0B phosphotransferase, and the Rap phosphatases. How Spo0F maintains specificity of interaction with such an array of proteins is an interesting question of molecular recognition, especially considering the abundance

† This investigation was supported in part by Grants GM19416 and GM55594 from the National Institutes of Health. This is publication 11699-MEM from the Department of Molecular and Experimental Medicine at The Scripps Research Institute.

* To whom correspondence should be addressed. Tel: (619) 784-7905. Fax: (619) 784-7966. E-mail: hoch@scripps.edu.

‡ The Scripps Research Institute.

§ New York State Department of Health.

10.1021/bi981340o CCC: $15.00
Published on Web 11/06/1998

of two-component systems within a single cell (*12*, *13*). In an alanine-scanning mutagenesis study of Spo0F designed to delineate the surface residues of Spo0F responsible for interaction with its modifying proteins, several alanine substitutions gave genetic phenotypes best interpreted as resistant to the Rap phosphatases known to be specific for Spo0F∼P (*14*). Previous studies identified residue Y13 of Spo0F as important for RapA and RapB phosphatase interaction; substitution by serine at position Y13 imparts phosphatase resistance to Spo0F (*9*).

In this study, 16 Spo0F mutants with alanine-substituted residues potentially defining the Rap phosphatase interaction surface were assayed in vitro for sensitivity to RapB phosphatase. Additionally, the metal dependence of RapB-catalyzed dephosphorylation and the RapB activity in the presence of vanadate were characterized to distinguish between possible models for RapB activity.

MATERIALS AND METHODS

Bacterial Strains and Reagents. *E. coli* strains were maintained on Luria-Bertani medium supplemented with ampicillin at 100 μg/mL or chloramphenicol at 30 μg/mL. Strain DH5α was used for propagation and maintenance of plasmids and strain BL21(DE3)pLysS for protein expression. Transformations were performed by electroporation using gene pulser (Bio-Rad). Sequenase version 2.0 DNA Sequencing kit from Amersham and PAGE I sequencing gel kit (Boehringer Mannheim) were used for DNA sequence analysis. [γ-^{32}P]ATP (6000 Ci/mmol, 150 mCi/mL) was obtained from NEN Life Science Products, DuPont. Protein molecular weight markers were from Novex. Sodium orthovanadate was obtained from Sigma Co.

DNA Manipulation and Protein Purification. Cloning and site-directed mutagenesis were done as described previously (*14*). DNA sequence analysis was used to screen for clones containing the desired mutation, and the entire gene was subsequently sequenced to ensure no additional mutation existed. Expression of His-tagged proteins and purification to homogeneity were performed according to the described procedures (*14*). RapB protein with N-terminal 10xHis tag (in pET16b) (*9*) was also purified in a similar fashion and was concentrated by a Centricon-30 concentrator (Amicon). Protein concentration was determined by BCA protein assay (Pierce) with bovine serum albumin as a standard. Concentration of Spo0F was determined by its extinction coefficient (*15*).

Spo0F∼P Purification. $(His)_6$-tagged Spo0F (50 μM) was phosphorylated with KinA (0.5 μM) and [γ-^{32}P]ATP (1 mM at specific activity of 0.6 Ci/mmol) for 2 h as previously described (*14*). The reaction mixture (250 μL) was loaded onto a Ni−NTA spin column (Qiagen) with low-speed centrifugation (1700 rpm × 3 min). The column was washed twice with 500 μL of buffer containing 50 mM sodium phosphate, pH 8.0, 300 mM NaCl, and 10% glycerol. Retained protein was eluted by 150 mM EDTA[1] in the same buffer (300 μL × 3). Excess EDTA was removed by extensive dialysis in buffer S (50 mM sodium phosphate, pH 8.0, 50 mM KCl, 0.1 mM EDTA, and 10% glycerol) and protein was then concentrated by a Microcon-3 concentrator (Amicon).

Dephosphorylation Assays. Spo0F at a final concentration of 10 μM was phosphorylated by KinA (0.2 μM) and 0.4 mM [γ-^{32}P]ATP (6 Ci/mmol) for 40 min. At this point, any subsequent incorporation of radiolabel was minimized by adding 200-fold excess of unlabeled ATP. RapB was added 30 s after the addition of unlabeled ATP to a final concentration of 2 μM. The first sample was withdrawn after 15 s, mixed with 2× SDS electrophoresis loading buffer and frozen on dry ice. The radioactivity of Spo0F∼P in this sample was used as 100% in normalization. After completion of the time course, all samples were analyzed on a 15% Tris-tricine minigel. The gel was dried, without staining, under vacuum, and the radioactivity remaining as Spo0F∼P was quantified with a PhosphoImager (Molecular Dynamics Corp.).

The autodephosphorylation of purified Spo0F∼P (10 μM) was performed in buffer S. Stock solutions of $MgCl_2$, $MnCl_2$, $ZnCl_2$, $CaCl_2$ (25 mM), and Na_3VO_4 (100 mM) were prepared in 100 mM Tris-HCl, pH 8.0. Divalent metals were used at a final concentration of 5 mM, and vanadate was added to a final concentration of 20 mM when desired. Reactions (with 1 μM of RapB if needed) were initiated by adding Spo0F∼P and were quenched by 2× SDS loading buffer. Samples were analyzed as described above.

RESULTS

Multiple Residues in the Region of β1−α1 Loop and the N-Terminus of Helix α1 Confer Phosphatase Resistance When Mutated to Alanine. Previous genetic screening which identified the Spo0F Y13S mutation to be Rap phosphatase resistant provided initial insight into the possible location of the Spo0F−Rap interaction surface (*9*). Because the average molecular recognition surface between two interacting proteins has been estimated to range in area from 639 to 3228 Å^2 (*16*), Rap phosphatases are likely to employ a broader recognition area beyond this residue of Spo0F. If a residue only participates in phosphatase recognition, a mutation removing this interaction is likely to give rise to an increased pressure to sporulate, leading to a hypersporulation phenotype (*9*, *17*). However, a mutation giving phosphatase resistance would not manifest a hypersporulation phenotype if this mutation also impaired phosphoryl input from kinases. The majority of surface residues (57 of 79), when altered to alanine, did not change the sporulation phenotype of the cell, suggesting they do not participate in recognition for kinases, phosphatases, or the Spo0B phosphotransferase. Therefore, all of the mutant proteins showing altered sporulation from the previous alanine-scanning mutagenesis were assayed for Rap phosphatase sensitivity.

The lifetimes of the phosphorylated Spo0F alanine mutant proteins and the phosphorylated wild-type Spo0F in the presence of RapB phosphatase are shown in Figure 1A. A time course for wild-type Spo0F∼P autodephosphorylation is included for reference. Many mutations located on the β1-α1 loop and the N-terminus of helix α1 (see Figure 5) completely abrogate or significantly diminish RapB activity on Spo0F. Y13A, R16A, and L18A mutant proteins were

[1] Abbreviations: PCR, polymerase chain reaction; IPTG, isopropyl-β-thiogalactopyranoside; NTA, nitrilo-tri-acetic acid; SDS, sodium dodecyl sulfate; PAGE, polyacrylamide gel electrophoresis; EDTA, ethylenediaminetetraacetic acid; NMR, nuclear magnetic resonance.

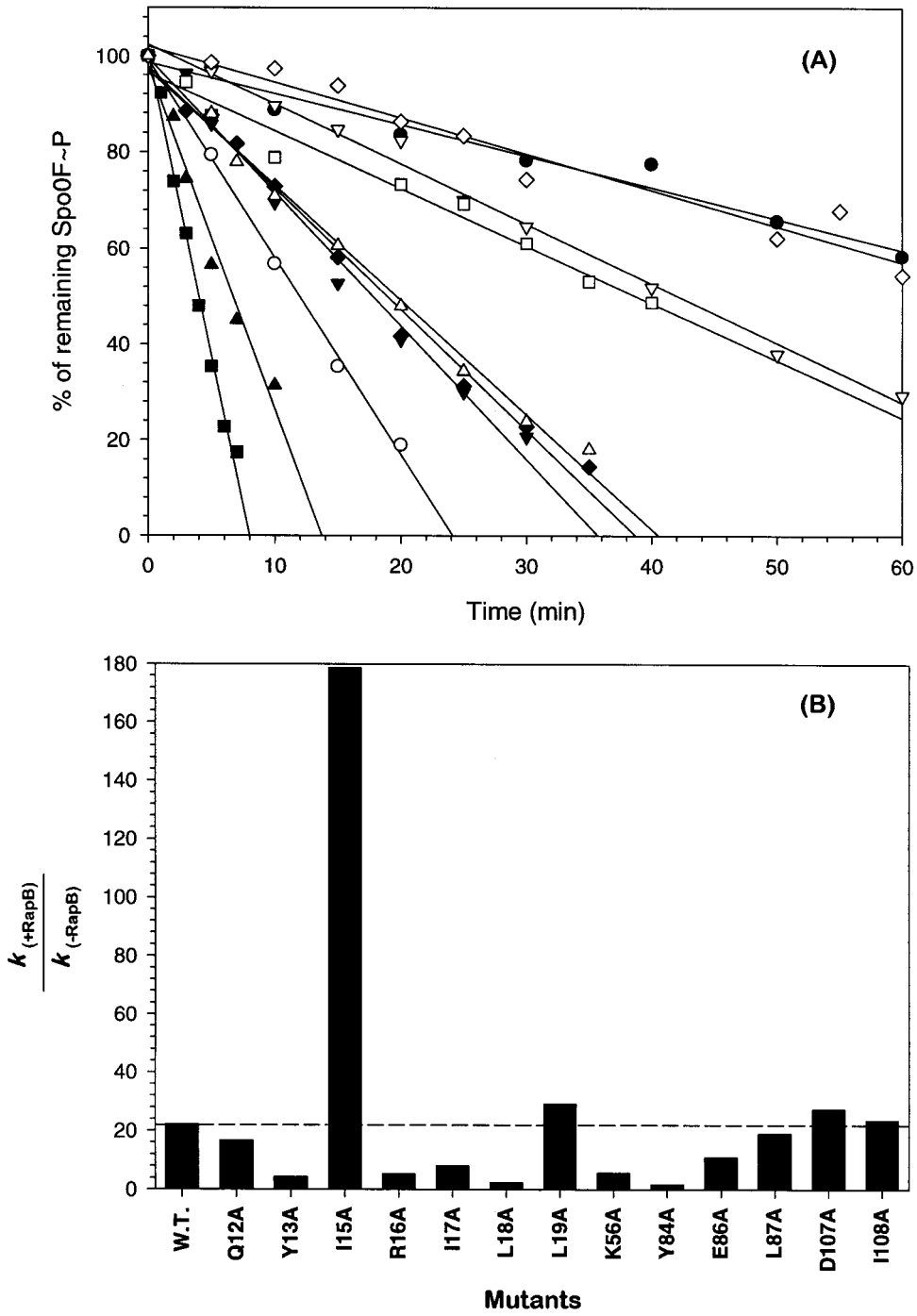

FIGURE 1: (A) RapB-catalyzed dephosphorylation reaction time course of Spo0F mutants. (●) Wild-type autodephosphorylation; (○) wild-type; (▼) Q12A; (▽) Y13A; (■) I15A; (□) R16A; (◆) I17A; (◇) L18A; (▲) L19A; (△) K56A. In vitro sensitivity to RapB phosphatase was investigated by reaction with Spo0F and RapB in a 5/1 ratio. This is one representative of at least two independent sets of experiments. (B) Fold of stimulation in dephosphorylation rate by RapB phosphatase. The ratio is calculated as the first-order rate constant in the presence of RapB divided by the rate constant of autodephosphorylation.

essentially resistant to RapB. Q12A and I17A mutant proteins gave RapB-dependent dephosphorylation rates intermediate between the wild-type autodephosphorylation rate and that of wild-type in the presence of RapB. Surprisingly, I15A and L19A mutant proteins showed enhanced reactivities to RapB. Proteins with mutant residues on two other loops, the $\beta4-\alpha4$ loop (Y84) and the $\beta3-\alpha3$ loop (K56), showed reduction in sensitivity to RapB and are discussed below. E86A, L87A, D107A, and I108A proteins with mutant residues located on the $\beta4-\alpha4$ loop and helix $\alpha5$ were unaffected in their sensitivity to RapB (data not shown).

The apparent rate shown in Figure 1A results from both the RapB-stimulated dephosphorylation and autophosphatase activity of Spo0F. However, altered sensitivity or resistance to Rap phosphatase did not correlate to the autodephosphorylation lifetime of mutant Spo0F~P proteins derived from the cold chase method (*14*) which is similar to the assay condition applied here. L19A and Y13A mutant proteins, for example, have nearly identical autodephosphorylation half-lives, yet their reactivities with RapB are completely different. The stimulation of the dephosphorylation rate by RapB can be estimated through the ratio of rate constants

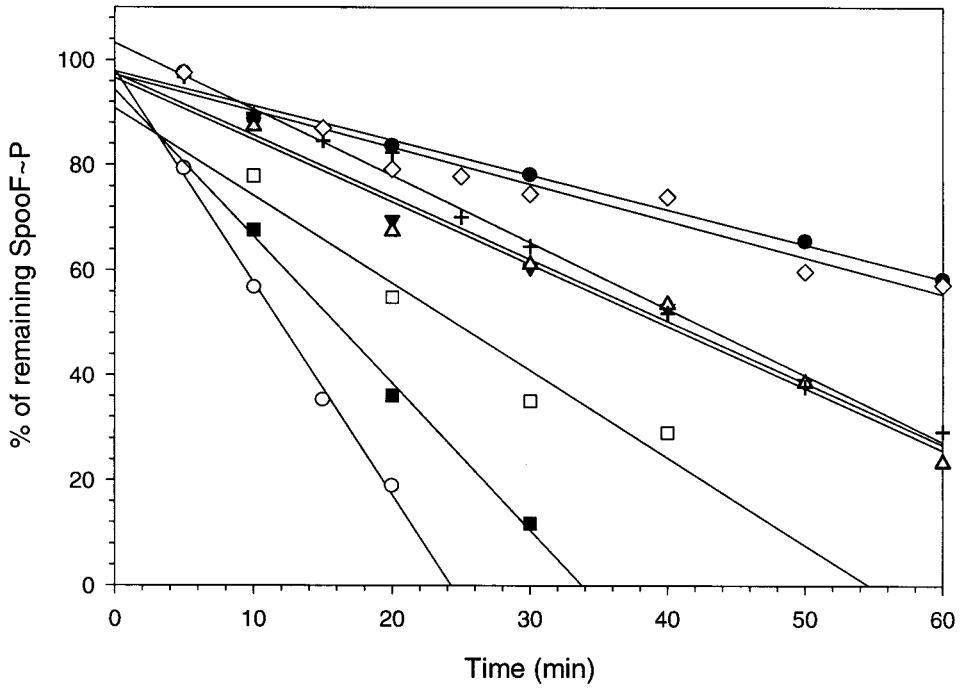

FIGURE 2: RapB reactivities of Spo0F Tyr13 mutants and Tyr84 mutants. (●) Wild-type autodephosphorylation; (○) wild-type; (▼) Y13W; (△) Y13S; (+) Y13A; (■) Y13F; (◇) Y84A; (□) Y84F. In vitro sensitivity to RapB phosphatase was investigated by reaction with Spo0F and RapB in a 5/1 ratio, and one set of experiments is shown ($n \geq 2$).

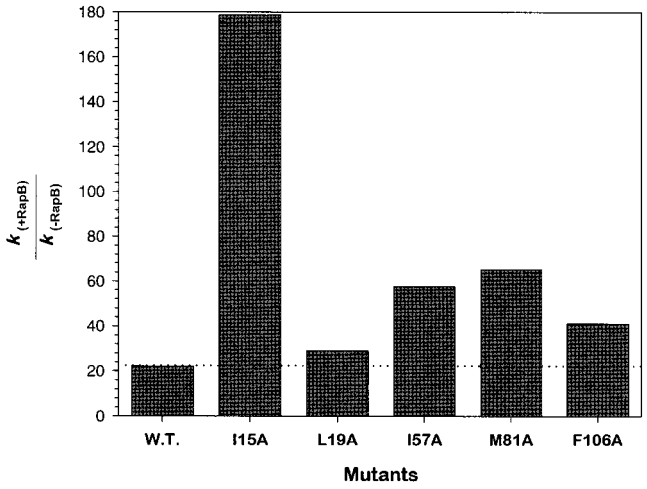

FIGURE 3: RapB sensitive mutation sites in Spo0F produced larger fold stimulation in dephosphorylation reactions than did wild-type protein.

obtained in the presence or absence of RapB (Figure 1B). When the autodephosphorylation rate was taken into account, RapB brought about a 22-fold enhancement in dephosphorylation rate of wild-type Spo0F. When the other mutant proteins were compared in this manner, the actual effect of the mutation on RapB phosphatase activity alone could be assessed. For example, the Q12A and L19A mutant proteins which were less sensitive or more sensitive, respectively, to RapB phosphatase gave much less significant effects than were apparent in Figure 1A while E86A and possibly L87A mutations whose proteins showed apparent unaltered wild-type RapB-dependent dephosphorylation rates (data not shown) were actually unable to be stimulated by RapB phosphatase to the same extent as the wild-type protein (Figure 1B).

The responses of mutant proteins toward RapB also did not correlate with their reactivities toward KinA~P and Spo0B~P. Both I15A and L18A mutant proteins exhibited similar reaction patterns to KinA~P and Spo0B~P (*14*), yet their responses to RapB were opposite.

Y13 and Y84 Residues May be Involved in Hydrophobic Contacts between Spo0F and RapB. In vitro studies have shown that the Y13S Spo0F mutation has no effect on the catalytic function of Spo0F but is critical to phosphatase recognition (*9*). Comparisons of the wild-type and Y13S mutant structures show that mutation of this surface-exposed residue has no overall structural consequences (*18*−*20*). Two types of interactions can be mediated through the side chain of a tyrosine residue: hydrogen bonding with the phenolic −OH group and hydrophobic packing with the aromatic ring. To better understand the nature of this interaction, site-directed mutagenesis was carried out to replace Y13 with phenylalanine and tryptophan. These Spo0F mutant proteins and the Y13S mutant proteins have normal phosphotransfer activities with respect to KinA~P and Spo0B~P (data not shown). However, only the Y13F mutant protein retained substantial sensitivity to RapB, while Y13A, Y13S, and Y13W mutant proteins were mostly resistant to RapB (Figure 2). Under the reaction conditions used, the phosphoryl group of wild-type Spo0F~P was ~80% hydrolyzed after 20 min; the corresponding values for Y13F and all other mutant proteins were 65 and ~30%, respectively. Autohydrolysis of Spo0F~P after 20 min was about 10% (Figure 2). The relative sensitivities of these mutants toward the RapB phosphatase suggest that the hydrophobic phenyl ring of tyrosine, but not the hydroxyl group, is required for recognition and/or stabilization of the bound complex. The indole ring of tryptophan does not substitute.

A second solvent-exposed tyrosine residue Y84 adjacent to the active-site pocket is located on the opposite side of the active site from Y13. Similar to Y13, Y84 is situated on a mobile loop ($\beta4-\alpha4$) enclosing the active site. Although the Y84A mutation exhibited a sporulation-

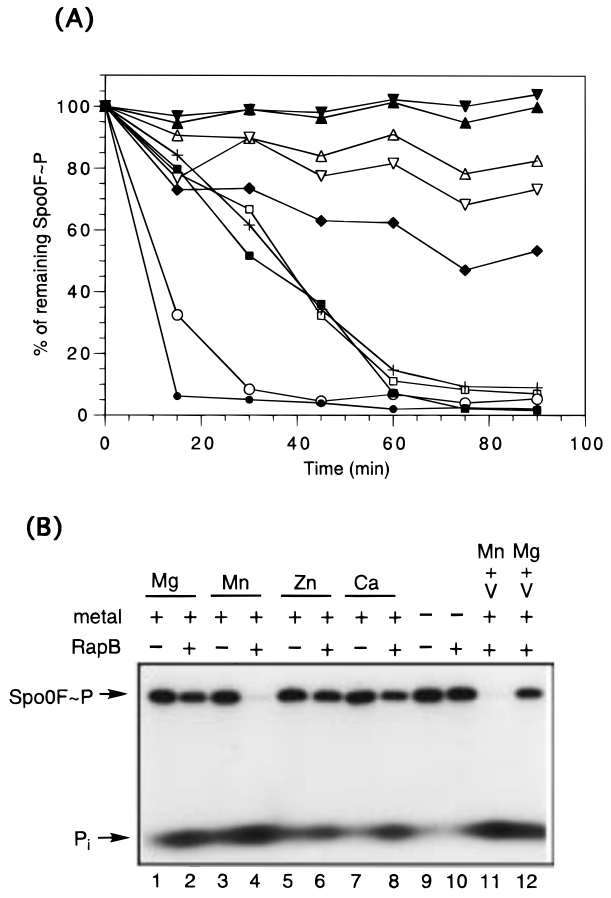

FIGURE 4: Metal ion preference for RapB catalyzed dephosphorylation. Reaction conditions are described in Methods and Materials. (A) Reaction time course. (▼) Spo0F∼P alone; (▲) Spo0F∼P + RapB; (△) Spo0F∼P + Mg^{2+}; (▽) Spo0F∼P + Mn^{2+}; (◆) Spo0F∼P + RapB + Zn^{2+}; (+) Spo0F∼P + RapB + Ca^{2+}; (□) Spo0F∼P + RapB + Mg^{2+}; (○) Spo0F∼P + RapB + Mn^{2+}; (■) Spo0F∼P + RapB + Mg^{2+} + Na_3VO_4; (●) Spo0F∼P + RapB + Mn^{2+} + Na_3VO_4. (B) An autoradiogram of the 30 min reaction.

deficient phenotype in vivo due to disruption of Spo0F−KinA interaction (*14*), the involvement of its phenolic side chain in RapB interaction was examined. Phenylalanine substitution at residue Y84 has only a moderate effect on RapB-catalyzed dephosphorylation when compared to a Y84A mutation (Figure 2). This observation again suggests that this particular aromatic ring, rather than the hydroxyl group, is essential for RapB recognition. However, the autodephosphorylation rate of Y84F was not tested and a decreased rate would affect this conclusion. Removal of the hydroxyl on residue 84 severely affects KinA reactivity and leads to a sporulation-deficient phenotype (data not shown).

The K56A Mutation Influences RapB-Catalyzed Spo0F∼P Dephosphorylation. Lysine 56, located on the loop immediately following the site of phosphorylation (D54), has been suggested to be one of the important determinants of the autohydrolysis rate of Spo0F∼P (*19*). The rate of autohydrolysis was increased significantly when this residue was mutated to Asn, but only moderately when substituted by alanine (*21*). When assayed with RapB, the K56A mutant protein showed a reaction time course similar to those of Q12A and I17A mutant proteins (Figure 1A), and it conferred RapB resistance similar to that of the R16A mutant protein (Figure 1B). Mutation of lysine 56 may enhance metal binding by subtly changing the position of the backbone carbonyl important for magnesium coordination and/or it may remove an important salt bridge for stabilization of the acyl-phosphate resulting in an enhanced autodephosphorylation rate (*9*, *18*−*20*). Despite the increased autodephosphorylation rate for K56A, RapB is not able to achieve wild-type levels of dephosphorylation, suggesting that K56 plays a role in RapB catalyzed hydrolysis.

Buried, Nonpolar Residues near the Active Site Enhance Dephosphorylation Rates When Truncated. Additional alanine mutant proteins besides those with I15A and L19A mutations were observed to be dephosphorylated by RapB faster than wild-type protein (Figure 3). The unusually large stimulation of the I15A mutant is the result of its much diminished autodephosphorylation rate (*14*). Proteins altered in three other residues, I57, M81, and F106, which possess predominantly buried nonpolar side chains were also dephosphorylated at increased rates by RapB when their side chains were truncated. The proximity of these rate-enhancing mutants to the active site and their lack of surface accessibility suggests that these residues may not directly interact with the RapB phosphatase. Instead, the side-chain truncation of these residues to a methyl group may structurally alter the active site to destabilize the acyl-phosphate and/or facilitate nucleophilic attack by water on the phosphoryl group. The isolation of such mutants suggests that RapB may catalyze Spo0F dephosphorylation through an allosteric mechanism that alters the active-site conformation.

RapB Dephosphorylation of Spo0F Requires Divalent Metal Ions. The metal requirement for Spo0F∼P autodephosphorylation has been previously studied; the autodephosphorylation rate was maximum at 2 mM Mg^{2+} (*15*). In addition, Spo0F∼P has a higher affinity for Mn^{2+} (K_d 0.1−1.0 mM) than Ca^{2+} (K_d 2 mM) or Mg^{2+} (K_d 2 mM) as measured by fluorescence quenching of the Spo0F/Y13W protein (ref *21* and unpublished results). If RapB catalyzes Spo0F∼P hydrolysis through a mechanism similar to the autophosphatase reaction, a similar metal ion dependence would be expected. To test this possibility, Spo0F∼P was purified free of the Mg^{2+} used in the standard phosphorylation reaction by a Ni-NTA column that employed excess EDTA rather than imidazole to chelate metal ions and elute the protein. EDTA was subsequently removed through extensive dialysis. When purified wild-type Spo0F∼P was incubated at room temperature for 90 min, moderate hydrolysis was only detected after divalent ions were added back into the reaction mixture (Figure 4A). When purified Spo0F∼P was treated with RapB in the absence of metal ions, very little, if any, hydrolysis was detected after 90 min of incubation (Figure 4A), indicating that divalent metal ions are essential for dephosphorylation by RapB. In the presence of different metal ions, however, RapB accelerated Spo0F∼P hydrolysis and the reaction appeared to be metal dependent, exhibiting a preference of $Mn^{2+} > Mg^{2+} \approx Ca^{2+} > Zn^{2+}$. The higher catalytic efficiency of Mn^{2+} over Mg^{2+} correlates with its higher affinity for Spo0F protein. Ca^{2+} ion, which binds to Spo0F with the same affinity as Mg^{2+}, has activity similar to that of Mg^{2+}. Finally, vanadate, an inhibitor of phospho-intermediate generating enzymes such as phosphotyrosine phosphatases (*22*), did not inhibit either Mn^{2+}- or Mg^{2+}-catalyzed activities of RapB (Figure 4A and lanes 11 and 12 in Figure 4B).

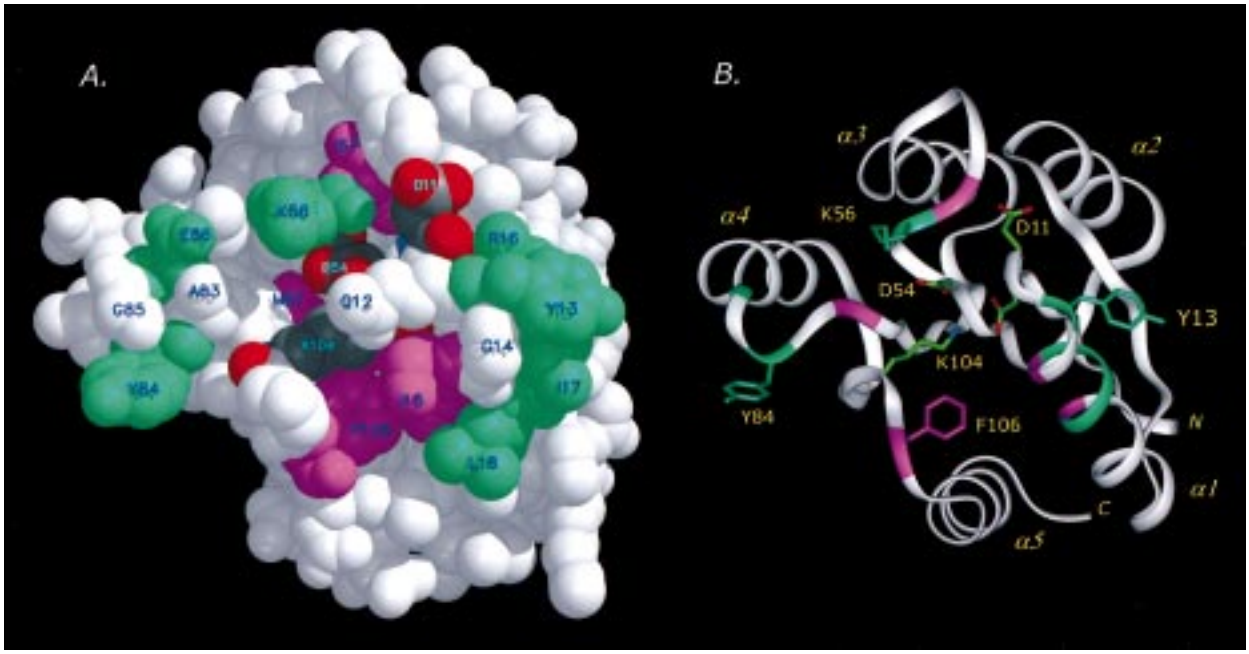

FIGURE 5: Distribution of residues affecting RapB activity mapped on the Spo0F structure. Residues resulting in strong RapB resistance upon mutation are colored in green, and those that show enhanced reactivity are colored in magenta. Residues Q12 and L19, which yield only moderate effect, remain uncolored. (A) Space-filled model. (B) Ribbon diagram shown in the same orientation as (A). This figure was generated by program MIDAS (A) and INSIGHT II (B).

DISCUSSION

Using site-directed mutagenesis and in vitro assays, this study provides a more detailed view of the Spo0F residues that are critical in Spo0F−RapB interactions. The 16 alanine mutations studied were known from an earlier study to alter sporulation frequency. These mutations are located on loops surrounding the aspartyl pocket (β1−α1, β3−α3, and β4−α4) and the N-terminal regions of helices α1, α4, and α5. The surface-filling model illustrated in Figure 5 shows that the residues giving RapB resistance form a mostly hydrophobic surface surrounding the D54 site of phosphorylation that may be largely responsible for stabilizing the RapB:Spo0F complex. This surface is likely also to be used by RapA because these two phosphatases share a high degree of sequence homology (*23*). Five alanine mutants (I15A, L19A, I57A, M81A, and F106A) demonstrated enhanced RapB dephosphorylation rates compared to wild-type RapB:Spo0F∼P hydrolysis. These residues also cluster around the D54 site of phosphorylation and are hydrophobic, yet differ from the RapB resistant mutants because they are mostly buried. Each of these hydrophobic residues is highly conserved throughout response regulator proteins and have previously been suggested to be important in the structural core of this family of proteins (*24*). Thus, the consequence of these mutations may be structural changes, which disrupt the aspartyl pocket, thereby enhancing RapB induced hydrolysis of the acyl-phosphate.

It is believed that all two-component response regulators share similar secondary structure organization; therefore, sequence comparison provides valuable information about relevant functional roles of certain residues. Conserved residues revealed by sequence alignment suggest their potential roles in structural folding and/or reaction mechanisms. The active-site residues forming the "aspartyl pocket" and the conserved hydrophobic residues in this family are clear examples (*25*). On the other hand, nonconserved residues identified in functional analysis provide insight toward specificity for protein:protein and/or protein:ligand interactions; these residues are more likely to locate on the surface of the protein. However, residues participating in both molecular recognition and catalytic function are possible.

With the completion of the *B. subtilis* genome sequencing project, 34 response regulators have been identified through sequence homology analysis (*12*). Sequence alignment of these response regulators revealed some interesting characteristics of Spo0F residues mentioned above. All residues essential for RapB activity are surface exposed and are not well conserved (except for the moderately conserved R16 and L18). In particular, tyrosine 13 of Spo0F is unique at this position of the β1−α1 loop; no tyrosines and only one phenylalanine are found in equivalent sites of other response regulators. This is well correlated with the fact that RapB is a phosphatase which is believed to specifically dephosphorylate Spo0F∼P. The other response regulator in the phosphorelay, Spo0A, is not a substrate of Rap phosphatases (*9*). Consequently, the putative determinants for RapB recognition may be absent in Spo0A. A direct comparison of RapB-resistant Spo0F residues to Spo0A through sequence alignment is Q12:N12, Y13:R13, R16:V16, I17:S17, L18:L18, K56:I58, Y84:F88, and E86:Q90; clearly providing enough differences for defining specificity. Most notably, the corresponding residue of Y13 of Spo0F in Spo0A is R13, a charged and bulkier functional group as compared to tyrosine.

The remaining surface-exposed and relatively unconserved residues causing altered RapB activity upon alanine substitution are Q12, I17, K56, and E86. It is not clear at this point whether the first two directly engage in RapB recognition or if they induce conformational changes of the critical residues as they are immediately adjacent to Y13 and R16. Particularly, the phenyl ring of Y13 is resting on top of the

side chain of I17 in the crystal structure (*18*). Truncation of I17 may therefore remove this favorable hydrophobic interaction and cause structural and dynamic changes in the N-terminus of helix α1 and the preceding loop. In the case of K56A, it is conceivable that this residue would participate in dephosphorylation by RapB, since K56 partially shields the active site from solvent.

Other putative RapB-interacting residues, R16 and L18, are relatively conserved in the response regulator family [42 and 52% (L + I + M), respectively]. Conservation of an arginine at residue 16 of Spo0F has been attributed to its aliphatic methylene side chain being the hydrophobic cover of the α1−β1 interface (*25*). The guanidinium group, however, could also have a unique functional role as discussed later. The side chain of L18 on helix α1 has hydrophobic contacts with I108 on helix α5 and may be important for maintaining the α1−α5 interface of Spo0F. Reducing the butyl group of L18, but not that of I108, to a methyl group causes the resistance to RapB. This resistance of L18A is, therefore, likely due to specific molecular recognition, not to nonspecific structural perturbations.

The RapB hypersensitive residues are highly conserved residues among *B. subtilis* response regulators with respect to their size and polarity, further supporting the notion that they are involved in maintaining the structural integrity of the active-site skeleton. For example, either leucine or methionine, which have the same van der Waals volume as isoleucine, always occupies a position equivalent to I57 in response regulators. The exclusive existence of such hydrophobic amino acids at this position has been suggested to be part of the invariable γ-loop (*25*) that may play a role in orienting the aspartate side chain of D54 into a more stable local environment once phosphorylated. Analogously, F106 and L19 may be involved in the positioning of the other active-site residue K104.

Several mutants of CheY, the chemotactic response regulator, have been identified to give resistance to CheZ, a phosphatase which shares no amino acid sequence homology to the Rap phosphatases (*26*, *27*). These phosphatase-resistant mutations of CheY are located on α1, further down the helix than those identified in Spo0F, and all carry charge alterations. One mutation introduces a new negative charge (N23D), and the others involve positive−negative charge swapping (K26E and E27K). Therefore, certain electrostatic interactions between CheY and CheZ were presumably disrupted. Additionally, a mutation at the active-site residue K109 of CheY (K109R) also gives rise to CheZ resistance. On the contrary, our study illustrates that resistance of Spo0F∼P to RapB is generated through truncating side chains of residues, mostly neutral, to alanine. All of these residues are surface exposed and are likely to interact with RapB through hydrophobic and/or hydrogen-bonding interactions. The general locations for phosphatase interaction are similar in Spo0F and CheY, yet quite different functional group substitutions confer resistance. RapB and CheZ are completely different proteins carrying the same enzymatic activity. It is conceivable that different phosphatases utilize divergent means of interaction in order to distinguish various phosphorylated cellular proteins.

Comparisons between bacterial response regulators and Ras protein have been made previously (*28*) because both protein families function as secondary messengers in signal transduction systems and because the phosphoanhydride bond of response regulator acyl-phosphate is analogous to the high-energy $O_\beta-P_\gamma$ bond of Ras-bound GTP. The recently solved crystal structure of the complex between Ras·GDP and a catalytic fragment of GAP and the reported mechanism for GAP-catalyzed GTP hydrolysis (*29*) provide additional grounds for expanding these comparisons to Spo0F:RapB interactions. GAP phosphatase abbreviates the "on" state of Ras by a factor of 10^5 by accelerating the slow intrinsic rate of GTP hydrolysis (*29*). GAP accomplishes this task through providing a critical catalytic arginine residue and restraining certain conformations of Ras by which the transition state of GTP hydrolysis is stabilized (*30*). An equivalent arginine is intrinsic to the α subunit of trimeric G protein, which has a GTPase activity ∼150-fold higher than does Ras (*31*). This observation argues that the guanidinium group has comparable roles in the two signaling proteins that utilize GTP hydrolysis. A phosphate−arginine interaction has also been suggested in serine/threonine phosphatase 2C, phosphotyrosine phosphatases, and acylphosphatases that hydrolyze carboxyl−phosphate bond of acyl-phosphate metabolites (*32*, *33*).

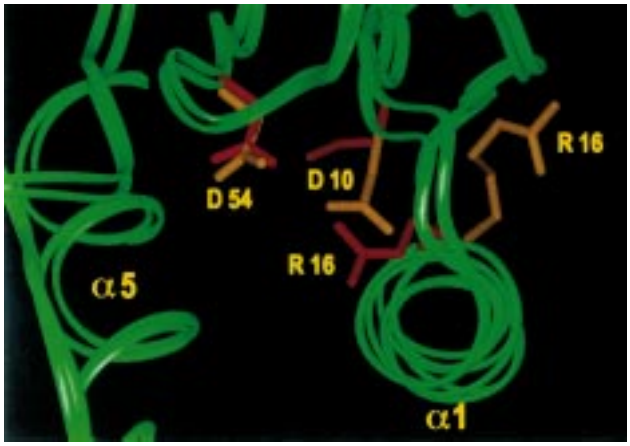

FIGURE 6: Multiple conformers of R16 on Spo0F. Two Cα backbone ribbon representations of the Spo0F family of solution structures (ref *13*; Brookhaven number: 1FSP) illustrate multiple conformers of the R16 side chain of helix α1. Three R16 conformers are observed, (1) the guanidinium group is solvent exposed (orange), (2) the guanidinium group is directed toward the aspartyl pocket (red), and (3) the guanidinium group is directed at the backbone carbonyl of D11 (not shown). The residue most affected by these multiple positions is the relative position of D10. Illustration was generated using INSIGHT (MSI software) and Photoshop version 4.0 (Adobe).

The role of Spo0F's R16 in RapB catalysis may be analogous to that of GTP hydrolysis by Ras proteins. R16 is very mobile according to NMR relaxation experiments and is observed to populate several conformations in the family of Spo0F structures determined by NMR (*20*). One set of structures shows the R16 guanidinium group in hydrogen bond distance of the backbone carbonyl of D10 and D11 (2.1−3.4 Å), and another set shows this guanidinium group in more solvent-exposed positions. In several structures, the R16 guanidinium group is able to extend into the aspartyl pocket itself, lending itself as a potential ligand for the acyl-phosphate (3.8−4.5 Å, Figure 6). Exchange between these positions does not appear to be sterically hindered from inspection of space-filling models of the structures, only the position of the D10 carboxylate must

move in order to accommodate the R16 guanidinium group. The positions of Y13 and I17 are also observed in multiple conformations; furthermore, the positions of I17, Y13, and R16 appear to influence one another, suggesting that these residues may behave in a concerted motion. RapB may operate partially through constraining the motion of the $\beta1-\alpha1$ loop, specifically Y13 residing in this loop, thereby influencing the conformation of R16, I17, and D10. Upon the formation of the RapB−Spo0F∼P complex, the guanidinium group could then adopt a conformation that stabilizes the transition state of acyl-phosphate hydrolysis, similar to that proposed in the GTP hydrolysis mechanism of Ras. Other interpretations of the R16A phenotype are equally plausible. For example, truncation of the arginine side chain may remove important protein:protein contacts between Spo0F and RapB, either those made directly with R16 or by introducing structural changes (e.g., the conformation of Y13 through I17 interaction) that prohibit RapB recognition.

An important factor in the ability of GAP to accelerate GTP hydrolysis is that it can confine a mobile region of Ras that contains a transition-state-stabilizing element (*30*). This interaction between Ras and GAP mainly consists of weak van der Waals and polar interactions. Two tyrosine residues (Y32 and Y64) of Ras, located on the two flexible switch regions, participate in the hydrophobic interactions. Y64F mutation of Ras has been shown to have no effect on the Ras−GAP interaction. The putative functional role of the $\beta1-\alpha1$ loop and possibly the $\beta4-\alpha4$ loop in RapB-catalyzed Spo0F∼P dephosphorylation is described here to mimic the switch regions of Ras protein. The dynamic characteristics of these two loops have been identified in NMR structural studies of Spo0F (*20*). Each contains a critical tyrosine residue (13 and 84, respectively) whose phenolic rings act as recognition "tags" for RapB or serve to stabilize protein: protein interactions.

Catalysis through allosteric interactions was proposed upon the identification of CheZ-resistant CheY mutations (*26*). As demonstrated on phosphotyrosine phosphatases, vanadate can serve as a transition-state analogue inhibitor if a phosphoenzyme intermediate is generated in the course of catalysis. The lack of inhibition by vanadate in RapB-catalyzed dephosphorylation implies that RapB does not directly participate in the release of phosphate. In other words, water would likely be the nucleophilic reagent while RapB functions as an auxiliary component. Considering that all RapB-hypersensitive mutations are in buried residues surrounding the active site and that autodephosphorylation and RapB-catalyzed dephosphorylation utilize metal ions similarly, catalysis by RapB phosphatase most likely occurs through promotion of Spo0F∼P conformational changes that accelerate autohydrolysis of phosphorylated Spo0F.

ACKNOWLEDGMENT

We thank Dr. James W. Zapf for providing Spo0FY13S and Spo0FY13W proteins.

REFERENCES

1. Burbulys, D., Trach, K. A., and Hoch, J. A. (1991) *Cell 64*, 545−552.
2. Parkinson, J. S., and Kofoid, E. C. (1992) *Annu. Rev. Genet. 26*, 71−112.
3. Trach, K. A., and Hoch, J. A. (1993) *Mol. Microbiol. 8*, 69−79.
4. Hoch, J. A. (1993) *Annu. Rev. Microbiol. 47*, 441−465.
5. Uhl, M. A., and Miller, J. F. (1996) *EMBO J. 15*, 1028−1036.
6. Posas, F., Wurgler-Murphy, S. M., Maeda, T., Witten, E. A., Thai, T. C., and Saito, J. (1996) *Cell 86*, 865−875.
7. Alex, L. A., Borkovich, K. A., and Simon, M. I. (1996) *Proc. Natl. Acad. Sci. U.S.A. 93*, 3416−3421.
8. Ohlsen, K. L., Grimsley, J. K., and Hoch, J. A. (1994) *Proc. Natl. Acad. Sci. U.S.A. 91*, 1756−1760.
9. Perego, M., Hanstein, C. G., Welsh, K. M., Djavakhishvili, T., Glaser, P., and Hoch, J. A. (1994) *Cell 79*, 1047−1055.
10. Wang, L., Grau, R., Perego, M., and Hoch, J. A. (1997) *Genes Dev. 11*, 2569−2579.
11. Perego, M., and Hoch, J. A. (1996) *Trends Genet. 12*, 97−101.
12. Kunst, F., et al. (1997) *Nature 390*, 249−256.
13. Mizuno, T. (1997) *DNA Res. 4*, 161−168.
14. Tzeng, Y.-L., and Hoch, J. A. (1997) *J. Mol. Biol. 272*, 200−212.
15. Zapf, J. W., Hoch, J. A., and Whiteley, J. M. (1996) *Biochemistry 35*, 2926−2933.
16. Jones, S., and Thornton, J. M. (1996) *Proc. Natl. Acad. Sci. U.S.A. 93*, 13−20.
17. Spiegelman, G., Van Hoy, B., Perego, M., Day, J., Trach, K. A., and Hoch, J. A. (1990) *J. Bacteriol. 172*, 5011−5019.
18. Madhusudan, Zapf, J. W., Hoch, J. A., Whiteley, J. A., Xuong, N. H., and Varughese, K. I. (1997) *Biochemistry 36*, 12739−12745.
19. Madhusudan, Zapf, J. W., Whiteley, J. M., Hoch, J. A., Xuong, N. H., and Varughese, K. I. (1996) *Structure 4*, 679−690.
20. Feher, V. A., Zapf, J. W., Hoch, J. A., Whiteley, J. M., McIntosh, L. P., Rance, M., Skelton, N. J., Dahlquist, F. W., and Cavanagh, J. (1997) *Biochemistry 36*, 10015−10025.
21. Zapf, J. W., Madhusudan, Grimshaw, C. E., Hoch, J. A., Varughese, K. I., and Whiteley, J. M. (1998) *Biochemistry 37*, 7725−7732.
22. Walton, K. M., and Dixon, J. E. (1993) *Annu. Rev. Biochem. 62*, 101−120.
23. Perego, M., Glaser, P., and Hoch, J. A. (1996) *Mol. Microbiol. 19*, 1151−1157.
24. Volz, K. (1995) in *Two-Component Signal Transduction* (Hoch, J. A., and Silhavy, T. J., Eds.) pp 53−64, ASM Press, Washington, DC.
25. Volz, K. (1993) *Biochemistry 32*, 11741−11753.
26. Sanna, M. G., Swanson, R. V., Bourret, R. B., and Simon, M. I. (1995) *Mol. Microbiol. 15*, 1069−1079.
27. Zhu, X., Rebello, J., Matsumura, P., and Volz, K. (1997) *J. Biol. Chem. 272*, 5000−5006.
28. Lukat, G. S., Lee, B. H., Mottonen, J. M., Stock, A. M., and Stock, J. B. (1991) *J. Biol. Chem. 266*, 8348−8354.
29. Gideon, P., John, J., Frech, M., Lautwein, A., Clark, R., Scheffler, J. E., and Wittinghofer, A. (1992) *Mol. Cell. Biol. 12*, 2050−2056.
30. Scheffzek, K., Ahmadian, M. R., Kabsch, W., Wiesmuller, L., Lautwein, A., Schmitz, F., and Wittinghofer, A. (1997) *Science 277*, 333−338.
31. Sprang, S. R. (1997) *Science 277*, 329−330.
32. Das, A., Helps, N. R., Cohen, P. T. W., and Barford, D. (1996) *EMBO J. 15*, 6798−6809.
33. Thunnissen, M. M., Taddei, N., Liguri, G., Ramponi, G., and Nordlund, P. (1997) *Structure 5*, 69−79.

BI981340O